

## Particulate morphology and elemental characteristics: variability at middle Indo-Gangetic Plain

V. Murari<sup>1</sup> · M. Kumar<sup>1</sup> · N. Singh<sup>1</sup> · R. S. Singh<sup>2</sup> ·  
T Banerjee<sup>1</sup>

Received: 18 May 2015 / Accepted: 29 September 2015 /

Published online: 5 October 2015

© Springer Science+Business Media Dordrecht 2015

**Abstract** Airborne particulates were monitored at an urban location of middle Indo-Gangetic Plain (IGP) and subsequently analyzed for particulate diversity and mixing states. Exceptionally high particulate loadings were found both in case of coarser ( $PM_{10}$ :  $157.5 \pm 102.9 \mu\text{gm}^{-3}$ ,  $n = 46$ ) and finer particulates ( $PM_{2.5}$ :  $92.5 \pm 49.8 \mu\text{gm}^{-3}$ ). Based on particulate morphology and elemental composition, five different clusters of particulates namely tarball, soot, sulphur-rich, aluminosilicate and mineral species were found to dominate. Soot particles ( $0.1\text{--}5 \mu\text{m}$ ) were found to be partly coated, having voids filled by coating material without being completely engulfed. A specific type of amorphous, carbonaceous spherules was evident in wintertime fine particulates signifying emissions from biomass burning and wild fire. Traces of S, Na and Ca were found associated with carbonaceous agglomerates suggesting its metal scavenging behavior. Particle laden filters were further processed for metallic and water soluble ionic species to constitute aerosol composition. Coarser particulates were characterized with higher metallic species (9.2–17.8 %), mostly of crustal origin (Ca: 5.5 %; Fe: 1.6 %; Zn: 1.3 % and Na: 3.8 %) while  $PM_{2.5}$  also revealed their association with metallic components (6.0–14.9 %) having Ca (4.6 %), Fe (0.9 %) and K (0.8 %) as principle constituents. Ca, Na and  $\text{NH}_4^+$  found to generate chloride and sulphate salts thus affecting particulate hygroscopicity. Elevated fractions of  $\text{NO}_3^-$  and  $\text{K}^+$  in  $PM_{2.5}$  signified contribution of biomass burning while presence of  $\text{Cl}^-$  with carbonaceous aerosols having traces of Si and K denoted contribution of farming and burning practices. Black carbon aerosol exhibited significant seasonal variability ( $6.9\text{--}21.9 \mu\text{gm}^{-3}$ ) which support larger association of carbonaceous aerosols in particle micrograph.

**Keywords** Aerosols · Electron-microscopy · Morphology · Mixing state · SEM-EDS · Indo-Gangetic Plain

✉ T Banerjee  
tb.iesd@bhu.ac.in; tirthankaronline@gmail.com

<sup>1</sup> Institute of Environment and Sustainable Development, Banaras Hindu University, Varanasi 221005, India

<sup>2</sup> Department of Chemical Engineering and Technology, Indian Institute of Technology - Banaras Hindu University, Varanasi, India

## 1 Introduction

Understanding specific behavior of airborne particulate in modifying regional climate remain a complication due to heterogeneities in particulate composition, morphology and mixing states (Ramanathan and Carmichael 2008; Banerjee et al. 2011a). Particle mass-size distribution and elemental composition are most fundamental properties that regulate its atmospheric behavior. Additionally, particulate morphology and mixing states are also relevant in assessing aerosol-climate interaction as morphology and mixing states essentially regulate particle optical and physio-chemical properties (China et al. 2013). Over the last decade, numerous scientific evidences have constituted association of airborne particulates with corresponding reduction in insolation (Xia et al. 2007), lower tropospheric heating (Guleria et al. 2014), changes in atmospheric thermal structure (Satheesh et al. 2009); deterioration in environmental quality (Banerjee and Srivastava 2011) and disruption of regional circulation systems (Ramanathan and Carmichael 2008). However, extent of such multi-lateral impacts with possible forecasting remain a complication and thus warrants specific investigation for region specific understanding.

Among few identified global aerosol hotspots, Indo-Gangetic plain (IGP) in south-east Asia comprising floodplain of the Indus and Ganges-Brahmaputra river system (Fig. 1) with nearly 1 billion of low-economy climate non-resilient population, is most vulnerable to climate induced severe, pervasive and irreversible impacts (IPCC 2013). The entire region is experiencing rapid change in land-use pattern associated to industrial and socio-economic development which consequently generate huge amount of continental

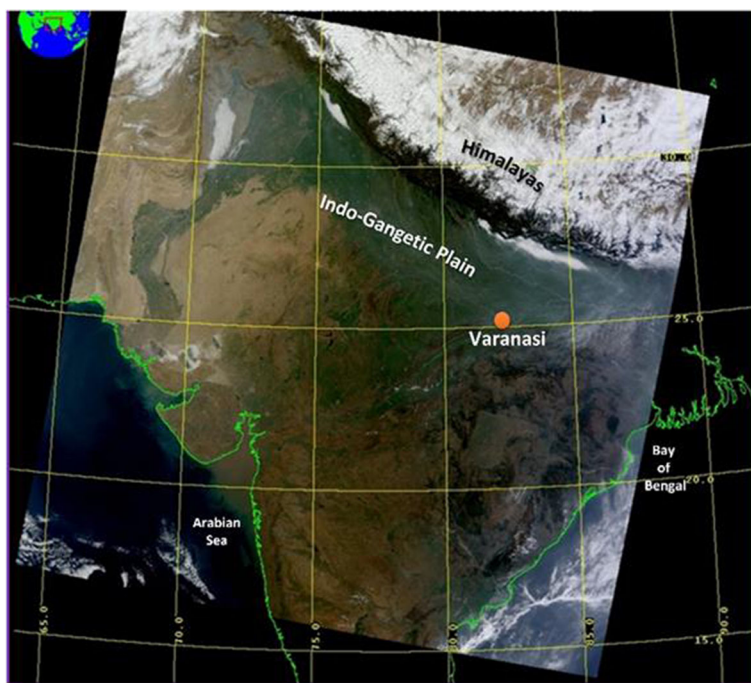


**Fig. 1** Geographical location of aerosol monitoring station at middle IGP. **Note:** Image downloaded from <http://ladsweb.nascom.nasa.gov/>

aerosols and their secondary products. Nature of aerosols at middle IGP is mostly characterized by dominance of organics (17–40 %), mineral dust (11–14 %) and ionic species (20–30 %) typically originated either from crustal resuspension, fuel combustions and wildfire (Murari et al. 2015). These local to regional sources occasionally supplemented with aerosols of transboundary origin predominately from Middle East countries and Great Indian Desert (Kumar et al. 2015; Sen et al. 2014). Therefore, existing particle diversity eventually generate an extremely complex heterogeneous aerosol system which require scientific understanding in terms of morphology, composition, size distribution, mixing state and chemical evolution.

For the present analysis, efforts were made to assess airborne particulate loading for both fine and coarse particulates at a ground based aerosol monitoring station in middle IGP. Individual particles were characterized for morphology, structure and mixing state through scanning electron microscope and subsequently analyzed through energy-dispersive X-ray spectrometry (SEM-EDS). Conclusively, particulates were further processed and analyzed for metallic content and water soluble ionic species to understand particle heterogeneity and complexity that exists within the region.

## 2 Experimental methods

### 2.1 Background of experimental site

Present experiment was carried out at Varanasi (25° 18'N, 82° 59'E), the religious capital of India and a true representative of middle-IGP in terms of climatology, topography and aerosol type (Fig. 1). Being a part of middle IGP, the city characteristically experiences humid sub-tropical climate with distinct seasonal variation viz. blazing summer (March to June, 38–42 °C), intense rainfall during monsoons (July to September, annual average 1100 mm, 80 % occurs in monsoon) and cold during winters (December to February, 7–15 °C) (Murari et al. 2015). Situated at western bank of river Ganga, the city comprises a very high population load with mixed residential and commercial sprawl surrounding the monitoring site. The sampling terrain was relatively flat without having any specific localized effect of oceans, mountains or explicit emission source. Synoptic wind pattern for the ground monitoring site was dominated by westerly during summer and winter while easterly during monsoon. For the current analysis, meteorological data including temperature and relative humidity (RH) were procured from web based database [wunderground.com](http://wunderground.com) and were further validated with ground based measurement. Atmospheric boundary layer depth (ABL) was procured from Global Data Assimilation System (GDAS, 1°, 3-hourly) collected from NOAA-ARL (<http://www.arl.noaa.gov/ready>; Draxler and Rolph 2003).

### 2.2 Particulate collection and analysis

Once in a week sampling of both fine and coarse particulates were continued from March to December, 2013 by means of dust samplers. Samplers were placed at a height of 7.5 m above ground and particulate sampling was continued for 24 h (1000–1000 h). For the current analysis, coarser particulates were collected through particulate sampler (IPM-FDS, Instrumex) with omni-directional ambient particle inlet having 10 µ separation assembly and coarser particulates were held deposited on glass fiber filter (GF/A, Whatman, 47-mm

diameter). Particulate sampler for PM<sub>10</sub> was run at an average airflow of 16.67 LPM (flow meter resolution of  $\pm 2\%$ ) while, fine particulate sampler (APM 550, Envirotech) was run at constant flow of  $1\text{ m}^3\text{h}^{-1}$  using polytetrafluoroethylene filters (PTFE, Whatman, 47-mm diameter). For fine particulate sampler, a WINS assembly with glass fiber filter immersed in silicon oil was specifically placed as impaction surface to segregate the particulates of desired aerodynamic diameter ( $\leq 2.5\ \mu\text{m}$ ). Exposed filters were placed into cassettes, wrapped in aluminum foil to prevent photo-degradation and subsequently gravimetrically analyzed after proper desiccation.

## 2.3 Quality control

Precautions were taken to ensure uniformity of particulate sampling for the entire monitoring period. Cleaning of impactor and changing of WINS-impactor filter paper were performed after every sampling to avoid any possible contamination. Flow rates of both particulate samplers were used to calibrate before every sampling through gas flow meter in order to avoid any possible leakage. Daily flow rate calculations were made to ensure fluctuations were within the range. Additionally, filter papers were equilibrated in desiccator at humidity (30–40 %) and temperature (20–30 °C) controlled environment for 24 h both before and after sampling. Filters were weighted thrice at a balance (AY220, Shimadzu) and exposed filters were stored under cool and dry condition (−20 °C) for further analysis. Both dust samplers have frequently being calibrated and blank filters were also processed by identical methods to reduce any bias.

## 2.4 Particle analysis by SEM-EDS

Morphological and elemental characterization of airborne particulates were performed by scanning electron microscope (JSM 6490LV, JEOL) coupled with Energy-dispersive X-ray spectroscopy (Oxford INCA x-act). Dry and particle loaded filters were cut in to the desired size (approx.  $1\text{ cm}^2$ ) and coated with gold (Au, <10 nm) by sputter in order to get better secondary images. Sample positioning, selection of analysis region and imaging were computer controlled. EDS spectra of airborne particles were further obtained through energy dispersive spectrometer with an accelerating voltage of 15–30 kV. Spectra were obtained at multiple points and elements were measured both qualitatively and quantitatively.

## 2.5 Chemical speciation of particulates

### 2.5.1 Trace metals

Aerosol samples were digested and extracted using US EPA Method IO-3.2 (EPA 1999). Filters were cut in an extracting solution containing HNO<sub>3</sub> (5.55 %) and HCl (16.67 %). Digested samples were filtered (No. 42, Whatman), diluted with de-ionized water and subsequently analyzed for metallic species by atomic absorption spectrophotometer (AAS, Avanta Ver 2.01, GBC). Similar procedure for extraction and analysis was made for blank filters in order to quantify background heavy metal concentrations. Details of sample digestion and extraction for metallic species have been given by Murari et al. (2015).

### 2.5.2 Water-soluble ionic constituents (WSIC)

Particle laden filter papers were initially ultrasonicated (Microclean-109, Oscar) for 90 min at 35 °C with de-ionized water for extraction of water-soluble inorganic species. Extracted samples were filtered through nylon filters (0.45  $\mu\text{m}$ , Millipore). Extraction and filtration of aerosol samples were followed by the analysis of their WSIC contents using ion chromatograph (IC, ICS-3000, Dionex, USA) having IonPac AS11-HC $\times$ 250-mm analytical column for anionic species and a separation column (IonPac CS17-HC, 4  $\times$  250 mm; Dionex, USA) for cations. Anionic species were analyzed using anion micro-membrane suppressor (ASRS-300, 4 mm; Dionex, USA) with IonPac analytical column having 20 mM NaOH (50 % w/w) as eluent and triple-distilled water as regenerator. Cations were detected using a suppressor (CSRS-300, Dionex, USA) with a separation column having 5 mM MSA (methane sulphonic acid) as eluent. Detailed instrumentation of Ion Chromatograph may found in the works of Murari et al. (2015).

### 2.5.3 Carbonaceous species

Carbonaceous species in terms of black carbon aerosols (BC) were measured in real time mode with a 7-channel aethalometer (AE-31, Magee Scientific, USA). Aethalometer was continuously operated during ground based aerosol monitoring period at a flow rate of 3.5 lpm and measured the reduction of beam of light at seven wavelengths i.e. 370, 470, 520, 590, 660, 880 and 950 nm. BC mass concentration measured at 880 nm was eventually considered for standard BC based on its maximum absorption capacity.

## 3 Results and discussion

### 3.1 Variability in PM<sub>10</sub>

Airborne particulate mass concentrations were continuously monitored during March to December, 2013 and entire particulate variability has been plotted in Figs. 2 and 3 with an indication of existing meteorological variables. Weekly average concentration of coarser

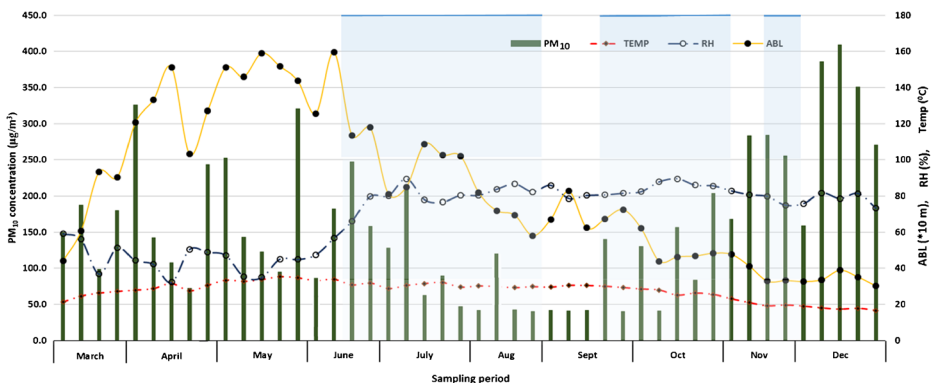


**Fig. 2** Time series of airborne PM<sub>10</sub> concentrations with meteorological variables. **Note:** Blue shades show rainy episodes

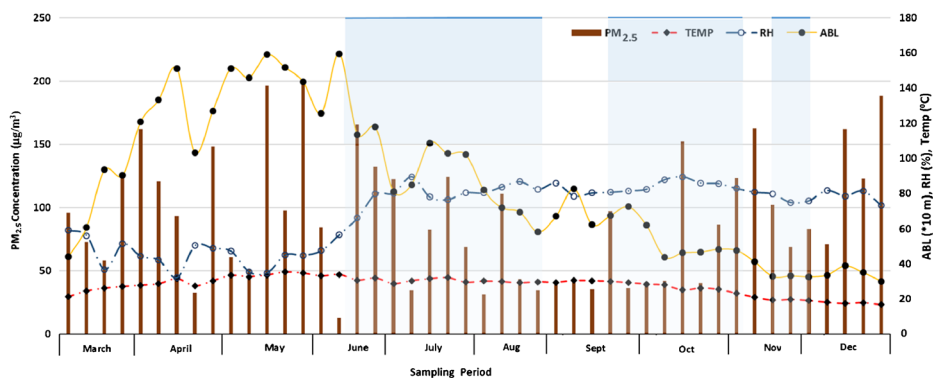


**Fig. 3** Time series of airborne  $PM_{2.5}$  concentrations with meteorological variables. **Note:** Blue shades show rainy episodes

particulate ( $PM_{10}$ , Fig. 2) for the entire monitoring period was  $157.5 \pm 102.9 \mu\text{g m}^{-3}$  (mean  $\pm$  sd) ( $n = 46$ ) with daily variation ranging from 12.4–409.3  $\mu\text{g m}^{-3}$ . Average  $PM_{10}$  mass concentrations exceeded the 24-h average standards of National Ambient Air Quality ( $100 \mu\text{g m}^{-3}$ , cpcb.nic.in) and USEPA standards ( $150 \mu\text{g m}^{-3}$ , <http://www.epa.gov/air>) which pose substantial threat to local habitat.

Coarser particulates revealed a clear seasonal trend having visible impacts of meteorological variables (Fig. 2). For the present analysis, particulate loading prevailed maximum during winter ( $285.1 \pm 87.1 \mu\text{g m}^{-3}$ ) possibly due to persistence of low atmospheric boundary layer height ( $36.1 \pm 5.5$  m) which reduce particulate dispersibility (Kumar et al. 2015). Characteristically, summer months also depict a high particulate loading ( $168.9 \pm 83.7 \mu\text{g m}^{-3}$ ) possibly due to particulate re-suspension from unpaved road and surrounding agricultural fields (Banerjee et al. 2011b, 2015). Interestingly, almost entire variability of coarser particulates (80.4 %) were found to be existing above a concentration range (40–45  $\mu\text{g m}^{-3}$ ) except monsoonal period which suggest persistence of a constant background concentration (40–45  $\mu\text{g m}^{-3}$ ) within the region. However, statistical analysis of long term particulate loading and its variation for the concerned middle IGP is under process for a more reliable estimate.

### 3.2 Variability in $PM_{2.5}$

Another point of interest for the current research was to assess background concentration of finer particulates ( $PM_{2.5}$ ). Extremely high fine particulate mass loading were evident at middle IGP with daily variation ranging from 12.8 to 198.8  $\mu\text{g m}^{-3}$  (Fig. 3) with summertime mean of  $106.0 \pm 54.1 \mu\text{g m}^{-3}$  having 77.8 % non-attainment of particulate standard (60.0  $\mu\text{g m}^{-3}$ ). Mean  $PM_{2.5}$  concentration ( $92.5 \pm 49.8 \mu\text{g m}^{-3}$ ,  $n = 46$ ) was well exceeding the national as well as USEPA (35.0  $\mu\text{g m}^{-3}$ ) standards. Finer particulate revealed significant seasonal variations with wintertime average of  $120.4 \pm 43.2 \mu\text{g m}^{-3}$  having 100 % of exceedence level ( $>60.0 \mu\text{g m}^{-3}$ ). Ironically, 67.4 % of  $PM_{2.5}$  sampling period exhibited violation of 24-h standards with 87 % concentrations persisting well above 35  $\mu\text{g m}^{-3}$  and rest fall within a level of 30–35  $\mu\text{g m}^{-3}$ .

Figure 4a, b denotes particulates seasonal variability both in terms of  $PM_{10}$  and  $PM_{2.5}$ . Higher mass loading of both type of particulates during winter (mean,  $PM_{10}$ :

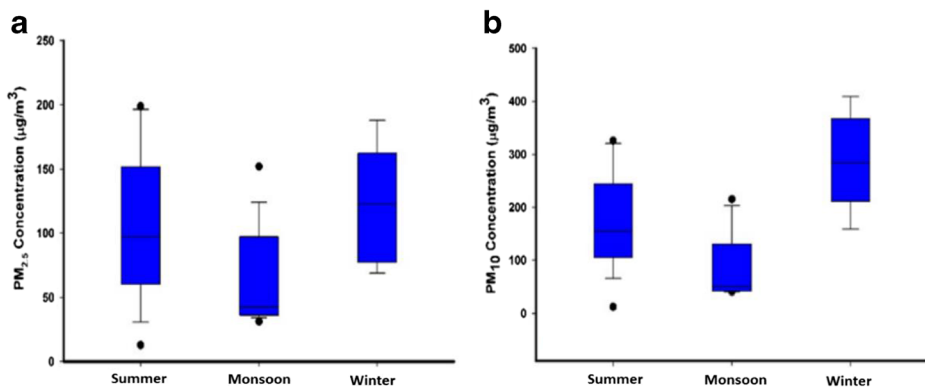


**Fig. 4** a, b Seasonal variations of airborne particulate at ground monitoring station

285.1;  $PM_{2.5}$ :  $120.4 \mu g m^{-3}$ ) and summer ( $PM_{10}$ : 168.9;  $PM_{2.5}$ :  $106.0 \mu g m^{-3}$ ) were clearly evident. Wintertime high particulate concentrations may well be explained by prevailing meteorology while summertime particulates possibly have crustal origin facilitated through reduced humidity and high wind speed (Banerjee et al. 2015). Both  $PM_{2.5}$  and  $PM_{10}$  exhibited an identical variation throughout the monitoring period and statistical analyses ( $R^2 = 0.29$ ,  $r = 0.54$ ) suggest somewhat similarity of their origin (Fig. 5).

### 3.3 Morphological characteristics of particulate

#### 3.3.1 S-rich particles

Sulphur rich particles (0.9–3.4 %) were found prevalent in both kind of particulates, while dominating in  $PM_{2.5}$  having size around  $2 \mu m$  (Fig. 6a). Interestingly, S-rich particles were predominately found to be associated with K, Ca, Mg, Al and sometime with Si. Association of S particles with Ca invariably suggests presence of Calcium Sulphate possibly originated either from crustal resuspensions or through conversion of

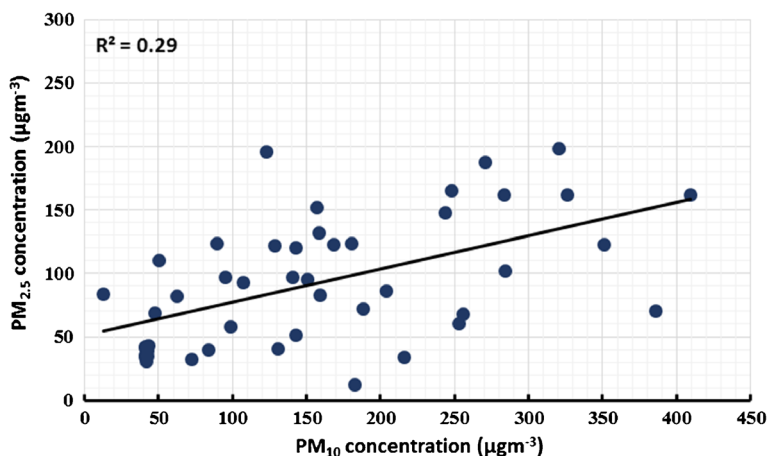


**Fig. 5** Ground level  $PM_{2.5}$  as a function of  $PM_{10}$



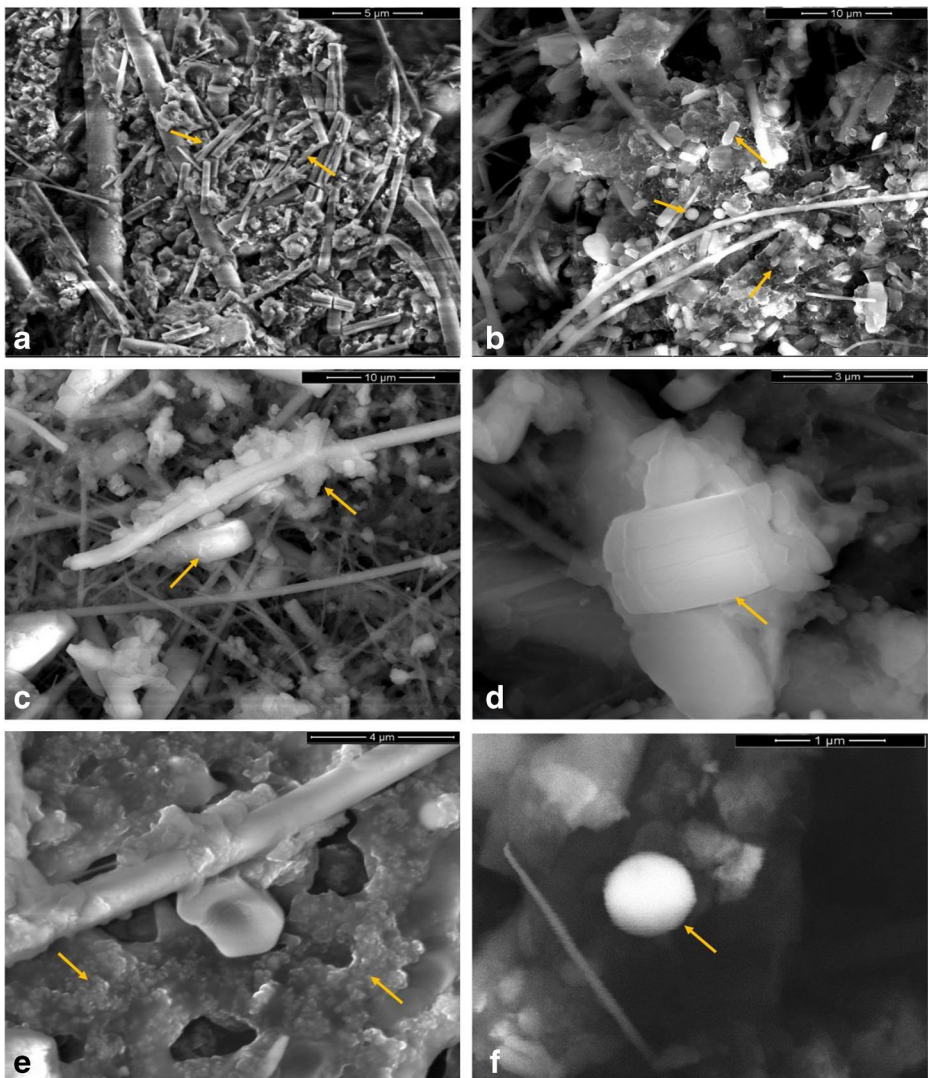


**Fig. 6** Micrographs of airborne particles with greater abundance at middle IGP **a** S-rich particles, mostly ammonium sulfates; **b, c** minerogenic particulates, mostly metal oxides of crustal origin, Silica, Ca/Mg carbonate; **d** aluminosilicates with spheroidal morphology; **e** ultrafine particulate of organic carbon or soot; **f** tarballs

calcite by reactions of sulphuric acid mists or ammonium sulphates (Cong et al. 2010). Association of S particles with K and Si indicate concurrent contribution of secondary aerosols from biomass burning and/or fossil fuel. In most of the cases, S particles were evident with irregular morphologies often with sharp edges. These aerosols have notable impacts on regional climate by essentially scattering the entire spectrum of solar radiation with a minute absorption in near infrared. Additionally, S particle make a complex mixture with other constituting elements, thus lead to uncertainties in terms of particle effective refractive index, morphology and hygroscopicity.



### 3.3.2 Minerals species

In our earlier submission, 12–14 % of particulate mass in middle IGP was found to be composed of mineral species (Murari et al. 2015). For the current analysis, minerogenic particulates (Fig. 6b, c) contribute proportion of PM<sub>10</sub> (10–15 %) while their abundance in PM<sub>2.5</sub> were relatively less (7–11 %). Among minerogenic species, Al, Si, Na and Ca were mostly dominant depicting significant correlation among themselves. For most instances, these minerogenic particles pose irregular shape (metal oxides of crustal origin, Silica, Ca/Mg, carbonate of soil origin, Fe and Ti rich particulates), while sometime having regular, rod like structure (CaSO<sub>4</sub>, Ca/Mg carbonate of anthropogenic origin, NaCl) or spheroidal with smooth texture (Iron oxides, calcium phosphate). Most of the metal oxides (mainly iron oxides) as of fly ash pose a definite spherical shape (Ebert et al. 2004), while for the present study was identified of having irregular morphology indicating their crustal origin (Cong et al. 2010).

### 3.3.3 Aluminosilicate

Both forms of particulates demonstrated deposition of Si (0–15.4 %), Al (0–3.7 %) and O-rich particles which signify the presence of aluminosilicates (Al + Si > 60 %) (Fig. 6d). These particles have origin associated with either combustion processes or from resuspensions of crustal material. For the current analysis, predominate proportion of aluminosilicate found to be non-spherical having sharp edges (dia. 1–8 μm) signifying their crustal origin. Naturally originated aluminosilicates mostly pose irregular shape as their evolution are associated with wind erosion of crustal surface. In contrast, some aluminosilicates were found to have spheroidal morphology enunciating origin related to high temperature combustion processes. These fine shaped particles (<2 μm) were typically anthropogenic fly ash, mostly dominant within PM<sub>2.5</sub>. Such explanations were in line of findings with other contemporary researchers like Ebert et al. (2004) and Cong et al. (2010). Interestingly, aluminosilicates were found to be associated with traces of toxic metal and chlorine compounds. Most aluminosilicates, Si, metal oxides within fly ash constituted a spherical shape with definite edges like structure having average granulometric spectrum of 0.5–2.0 μm.

### 3.3.4 Carbonaceous particles

Carbon rich particles exhibited highest abundance within fine range aerosol (0.5–1.5 μm) with typical aggregation of carbonaceous spherules (Fig. 6e). Based on morphology and visual estimation, most of soot particles were found to be partly coated having soot voids filled with coating materials without being completely engulfed. These carbon rich particles were morphologically well segregated from other typical aerosol constituents and pose spherical and chain like aggregates with granulometric size of 0.1–5 μm. Carbonaceous species found to be internally and externally mixed with other trace combustion particulates like sulphate, Si and K and in certain cases with crustal species (Ca, Na, Mg, K) suggesting its metal scavenging behavior (Pósfai et al. 2004).

### 3.3.5 Tarballs

Based on morphological and elemental composition, a specific type of carbonaceous particles ‘tarballs’ were recognized. Electron micrograph found these particles as amorphous and

spherical (Fig. 6f) without having any crystallographic structures as evident by China et al. (2013) and Pósfai et al. (2004). These ultrafine particles are specific subset of brown carbon and were mostly of <500 nm size while EDS spectra depicted predominant association of C and O with traces of K, S, Cl and Si. Particle composition and morphology confirmed presence of tarballs which were believed to be similar to high molecular weight humic like substances formed through gas to particle conversion process (China et al. 2013). Tarball mostly persisted without any visible aggregates, only externally mixed with other particles. Particulate tarballs play significant role in trapping insolation and, by extension, contribute in climate forcing and therefore, further investigations are in process to evaluate its mixing state and chemical evolution.

### 3.4 Morphological and elemental characteristics of particulates

#### 3.4.1 Morphological and elemental characteristics of $PM_{10}$

Essentially summertime particle micrographs were distinct from other seasons having high particulate deposition with irregular, crystal and fluffy shaped particles. In contrast, wintertime particulate micrograph indicated most notable deposition of irregular, flaky, crystal shape particles associated with more roundish, fluffy, amorphous shaped aggregates. Detail scanning denoted dominance of both spherulites with its clusters signifying presence of both minerogenic and carbon rich particles. Fly ash of aluminosilicate in nature having Al, Si and O rich species were ubiquitous in the coarser particulates. Being a part of IGP, it was obvious to find aluminosilicates as an aerosol component, but association of S possibly signify additional contribution from biomass/fuel combustion (Paoletti et al. 2003). Presence of unburnt hydrocarbons were further distinguishable with unique amorphous chain like spherulities having 0.5–2  $\mu\text{m}$  size, but were prominent within finer particulates.

Seasonal variation in  $PM_{10}$  elemental compositions were identified through SEM-EDS spectrum (Fig. 7a–c). Summertime particulates mostly found to be constituted with C–O rich

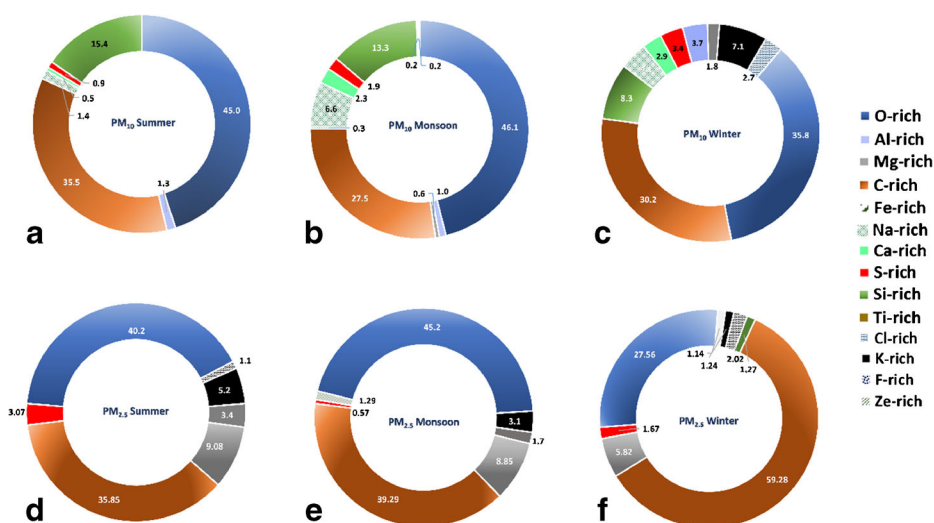


Fig. 7 a–f Variability in particulate elemental compositions at middle IGP

(80.5 %) and minerogenic particles (19.5 %). Wintertime aerosol resembled trend of having dominance with C and O-rich particles (>66.0 %) followed by Si(8.3 %), K(7.1 %), Na(4.1 %) and Al(3.7 %). Significant proportions of aerosol mass was found to be composed of carbonaceous species, predominately originated from fossil fuel combustion as implied by close association of C, O with S-rich (3.4 %) particles (Paoletti et al. 2003; Cong et al. 2010). Wintertime aerosol EDS spectra clearly identified association of K (7.1 %) with C and O particles which invariably suggest contribution from biomass burning, a common practice for local inhabitants (Murari et al. 2015). Presence of Cl (2.7 %) with carbonaceous aerosols having traces of Si and K denoted contribution of farming and burning practices, largely associated with regional livelihoods.

### 3.4.2 Morphological and elemental characteristics of PM<sub>2.5</sub>

Fine particle micrograph exhibited clear distinctions from coarser particulates having predominate deposition of fluffy, amorphous, flaky and chain like particles. The fluffy and amorphous deposition clearly evident the presence of carbonaceous spherules possibly originated from fuel combustions associated with traffic emissions and biomass burning. Carbonaceous spherules invariably dominated finer particulate morphology, however, further analysis revealed presence of both small aggregates of spherulites associated with its clusters.

Energy dispersive spectra (Fig. 7d–f) distinguished dominance of C, O and S-rich particles (79.1–88.5 %), while presence of F (5.8–9.1 %) may only be associated to industrial emissions (Pipal et al. 2014). Presence of F-rich particles were only evident within finer particulates with very few instances within coarser particulates. Wintertime particulate spectra revalidated the dominance of C and O-rich particles (>86.0 %) with traces of Cl (2.0 %) with Si (1.3 %) and K (1.2 %). Abundance of Cl spheroids with Si (1.3 %), K (1.2 %) and S (1.7 %) having size  $\leq 2.5$   $\mu\text{m}$  invariably suggest their farming and vegetation/coal burning origin. Sulphur-rich particles were common for both summer (3.1 %) and monsoon (0.6 %), while its abundance was higher during winter (1.7 %) associating K (1.2 %). In extremely humid condition, ultrafine particles having Cl and S possibly form agglomerates through gas-to-particle conversion of gaseous Cl with CaO and CaSO<sub>4</sub>. The groups of Ca (2.9 %) and Na (4.1 %) predominately having larger particle size (>2.0  $\mu\text{m}$ , Fig. 7c) and minerogenic origin reacts with gaseous Cl and reconstitutes chloride salts, thus affecting hygroscopicity of airborne particulates at middle-IGP.

## 3.5 Particle metal and WSIC constituents

Airborne coarse particulates at middle-IGP were further characterized through AAS and IC analysis for presence of metallic and ionic species. Seasonal variations in crustal originated metals were specifically observed for Ca (annual mean: 4.3 %; seasonal range: 4.1–7.2 %), Fe (1.6 %; 0.7–2.2 %), Zn (1.3 %; 0.6–1.9 %) followed by Na (3.8 %; 2.1–4.2 %) in respect to with other trace metals (1.8 %; 0.9–3.0 %) thus justifying particulate SEM-EDS spectra (Fig. 8a–c). The contributions of almost all metals to the PM<sub>10</sub> mass were usually found higher during winter except Ca (7.2 %), Fe (2.2 %) and Zn (1.9 %), which were higher during summer. Ionic constituents found contributing nearly 27 % of PM<sub>10</sub> mass while SO<sub>4</sub><sup>2-</sup> (8.0 %; 5.1–9.2 %), NH<sub>4</sub><sup>+</sup> (6.0 %; 4.2–8.7 %), NO<sub>3</sub><sup>-</sup> (7.0 %; 2.7–9.1 %) were the major ionic species followed by K<sup>+</sup> (2.5 %; 0.8–2.9 %), Cl<sup>-</sup> (2.4 %; 0.9–4.2 %), Mg<sup>+2</sup> (0.5 %; 0.4–1.2 %) and F<sup>-</sup> (0.4 %; 0.2–0.4 %) (Fig. 8d–f). Elevated fractions of NO<sub>3</sub><sup>-</sup> (9.1 %) and K<sup>+</sup> (2.9 %) during

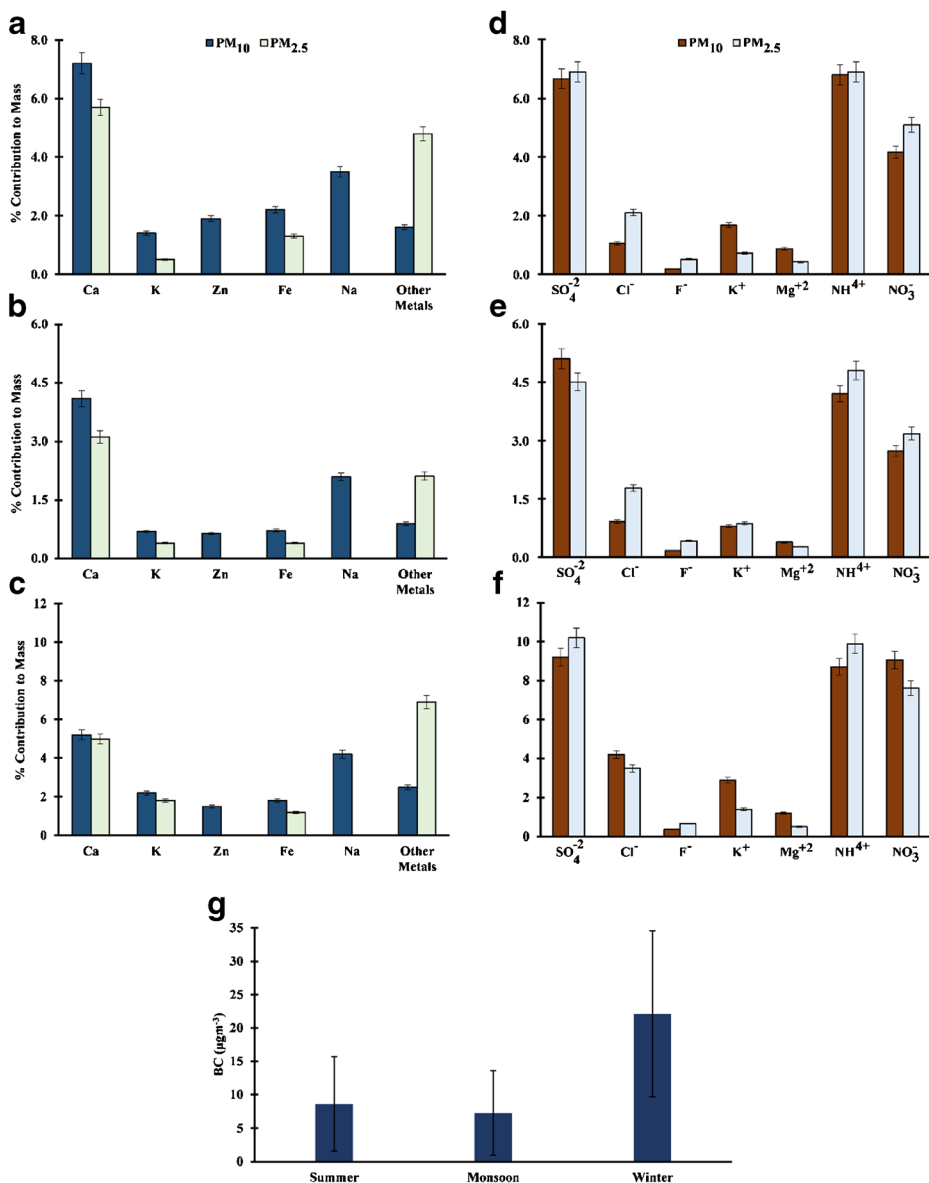


**Fig. 8** Seasonal variation in aerosol constituents at middle IGP; **a** summertime  $PM_{10}$ ; **b** monsoon  $PM_{10}$ ; **c** wintertime  $PM_{10}$ ; **d** summertime  $PM_{2.5}$ ; **e** monsoon  $PM_{2.5}$ ; **f** wintertime  $PM_{2.5}$ ; **g** black carbon

winter in comparison to summer ( $NO_3^-$ : 4.2 %;  $K^+$ : 1.7 %) and monsoon ( $NO_3^-$ : 2.7 %;  $K^+$ : 0.8 %) signify contribution of biomass burning and were in line with SEM-EDS spectra. In parallel, higher  $SO_4^{2-}$  fractions during winter was the product of low-volatility organic gases conversion and subsequent polymerization to aerosol particles (Pósfai et al. 2004). Higher  $NH_4^+$  fractions in winter aerosol signify the dominance of  $NH_3$  possibly originated from agricultural practices, livestock or through reduction of NO compounds in catalytic converters (Sharma et al. 2014).

PM<sub>2.5</sub> manifested presence of approximate 6.0–14.9 % metallic components predominately having Ca (annual mean: 3.2 %; seasonal range: 3.1–5.7 %), Fe (0.9 %; 0.4–1.3 %), K (0.8 %; 0.4–1.8 %) (Fig. 8a–c). For finer particulates, other trace metals also exhibited seasonal variation with metallic content varied from 2.12 % (monsoon) to 6.9 % (winters). Water soluble ions constituted a mass fraction (15.8–33.8 %) mostly contributed from SO<sub>4</sub><sup>2-</sup> (9.5 %; 4.5–10.2 %), NH<sub>4</sub><sup>+</sup> (8.2 %; 4.8–9.9 %), NO<sub>3</sub><sup>-</sup> (5.5 %; 3.18–7.62 %) and Cl<sup>-</sup> (2.6 %; 1.78–3.5 %). Higher fractions of ionic fluorides (as F<sup>-</sup>) in PM<sub>2.5</sub> during summer (0.51 %), monsoon (0.42 %) and winter (0.67 %) confirmed the presence of Fluoride rich particles in PM<sub>2.5</sub>.

Presence of a significant amount of black carbon aerosol and its associated seasonal variations in summer (9.3±3.0 μgm<sup>-3</sup>), monsoon (6.9±2.2 μgm<sup>-3</sup>) and winter (21.9±1.9 μgm<sup>-3</sup>) supported SEM micrograph interpretations and were in well agreement in terms of their differential seasonal pattern (Fig. 9). Higher black carbon mass concentration during winter invariably support wintertime particle micrograph which were mostly evident with association of spherical and chain like carbon aggregates.

## 4 Conclusions

Particulate morphology and mixing state characteristically regulate particle optical and physio-chemical behavior and therefore, modification in particle morphology and mixing state constitute significant uncertainties in assessing aerosol-climate interaction. For the present submission, efforts were made to identify temporal variation in airborne particulate morphology and mixing state for middle IGP and were substantiated with elemental characteristics. Principal findings of the research may be summarized as follows:

1. 63.0 % of PM<sub>10</sub> and 67.4 % of PM<sub>2.5</sub> sampling period exhibited non-attainment of particulate standards.
2. Based on SEM-EDS derived particle morphology, five clusters of particles namely tarballs, soot, S-rich particles, aluminosilicates and mineral species were found dominant in middle IGP.
3. S-rich particles (0.6–3.4 %) were found prevalent both in case of fine and coarse particulates, predominately associated with K, Ca, Mg, Al and sometime with Si.

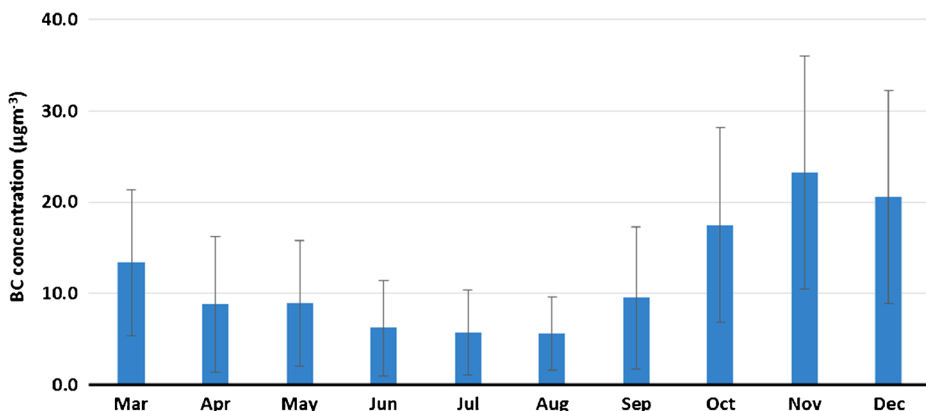


Fig. 9 Variation in monthly mean black carbon aerosol at middle IGP

4. Mineral species (Al, Si, Na and Ca) of crustal origin were mostly abundant in PM<sub>10</sub> (10–15 %) than PM<sub>2.5</sub> (7–11 %).
5. Soot particles (0.1–5 μm) were found constituted of carbonaceous spherules having an irregular morphology with spherical and chain like aggregates.
6. A specific type of amorphous, carbonaceous spherules were identified as tarballs signifying contribution of biomass burning on airborne particulates for middle IGP region.
7. The groups of Ca, Na and NH<sub>4</sub><sup>+</sup> found to constitute chloride and sulphate salts, thus affecting hygroscopicity of airborne particulates.
8. Sulphate, ammonium and nitrate were found to regulate WSIC chemistry in both fine and coarse particulates.
9. Presence of BC aerosol with significant wintertime concentrations supported larger association of carbonaceous aerosols in wintertime SEM particle micrograph.

**Acknowledgments** Particulate monitoring was financially supported by Department of Science and Technology, New Delhi (F. No. SR/FTP/ES-52/2014) and University Grants Commission, New Delhi (F. No. 41-1111/2012, SR) while BC was monitored under Aerosol Radiative Forcing over India (ARFI) scheme (Code: P-32-13) financed by Vikram Sarabhai Space Center, Indian Space Research Organization, Thiruvananthapuram. Authors duly acknowledge SEM-EDS facility provided by USIC-BB Ambedkar University, Lucknow and Department of Metallurgical Engineering, BHU, Varanasi. Guidance and cooperation provided by Director and Dean, IESD-BHU are also acknowledged.

## References

- Banerjee T., Srivastava R.K.: Evaluation of environmental impacts of Integrated Industrial Estate-Pantnagar through application of air and water quality indices. *Environ. Monit. Assess.* **172**(1–4), 547–560 (2011)
- Banerjee T., Barman S.C., Srivastava R.K.: Application of air pollution dispersion modeling for source-contribution assessment and model performance evaluation at integrated industrial estate-Pantnagar. *Environ. Pollut.* **159**, 865–875 (2011a)
- Banerjee T., Singh S.B., Srivastava R.K.: Development and performance evaluation of statistical models correlating air pollutants and meteorological variables at Pantnagar, India. *Atmos. Res.* **99**, 505–517 (2011b)
- Banerjee T., Murari V., Kumar M., Raju M.P.: Source apportionment of airborne particulates through receptor modeling: Indian scenario. *Atmos. Res.* **164–165**, 167–187 (2015)
- China S., Mazzoleni C., Gorkowski K., Aiken A.C., Dubey M.K.: Morphology and mixing state of individual freshly emitted wildfire carbonaceous particles. *Nat. Commun.* **4**, 2122 (2013). doi:10.1038/ncomms3122
- Cong Z., Kang S., Dong S., Liu X., Qin D.: Elemental and individual particle analysis of atmospheric aerosols from high Himalayas. *Environ. Monit. Assess.* **160**, 323–335 (2010)
- Draxler, R.R., Rolph, G.D.: HYSPLIT (Hybrid Single-Particle Lagrangian Integrated Trajectory) Model, <http://www.arl.noaa.gov/ready/hysplit4.html>, Accessed Oct 2014. (2003)
- Ebert M., Weinbruch S., Hoffmann P., Ortner H.M.: The chemical composition and complex refractive index of rural and urban influenced aerosols determined by individual particle analysis. *Atmos. Environ.* **38**, 6531–6545 (2004)
- EPA: Inventory of U.S. greenhouse gas emissions and sinks: 1990–2012. Environment Protection Agency (1999)
- Guleria R.P., Kuniyal J.C., Dhyani P.P., Joshi R., Sharma N.L.: Impact of aerosol on surface reaching solar irradiance over Mohal in the northwestern Himalaya, India. *J. Atmos. Sol. Terr. Phys.* **108**, 41–49 (2014)
- IPCC: In: Stocker T.F., Qin D., Plattner G.-K., Tignor M., Allen S.K., Boschung J., Nauels A., Xia Y., Bex V., Midgley P.M. (eds.) *Climate change 2013: the physical science basis. Contribution of Working Group I to the Fifth Assessment Report of the Intergovernmental Panel on Climate Change*. Cambridge University Press, Cambridge 1535 pp (2013)



- Kumar M., Tiwari S., Murari V., Singh A.K., Banerjee T.: Wintertime characteristics of aerosols at middle Indo-Gangetic Plain: impacts of regional meteorology and long range transport. *Atmos Environ.* **104**, 162–175 (2015)
- Murari V., Kumar M., Barman S.C., Banerjee T.: Temporal variability of MODIS aerosol optical depth and chemical characterization of airborne particulates in Varanasi, India. *Environ. Sci. Pollut. Res.* **22**, 1329–1343 (2015)
- Paoletti L., De Berardis B., Arrizza L., Passacantando M., Inglessis M., Mosca M.: Seasonal effects on the physico-chemical characteristics of PM<sub>2.5</sub> in Rome: a study by SEM and XPS. *Atmos. Environ.* **37**, 4869–4879 (2003)
- Pipal A.S., Jan R., Satsangi P.G., Tiwari S., Taneja A.: Study of surface morphology, elemental composition and origin of atmospheric aerosols (PM<sub>2.5</sub> and PM<sub>10</sub>) over Agra, India. *Aerosol. Air. Qual. Res.* **14**, 1685–1700 (2014)
- Pósfai M., Gelencsér A., Simonics R., Arató K., Li J., Hobbs P.V., Buseck P.R.: Atmospheric tar balls: Particles from biomass and biofuel burning. *J. Geophys. Res.-Atmos.* **109**, 1984–2012 (2004)
- Ramanathan V., Carmichael G.: Global and regional climate changes due to black carbon. *Nat. Geosci.* **1**, 221–227 (2008)
- Satheesh S.K., Vinoj V., Babu S.S., Moorthy K.K., Nair V.S.: Vertical distribution of aerosols over the east coast of India inferred from airborne LIDAR measurements. *Ann. Geophys.* **27**, 4157–4169 (2009)
- Sen A., Ahammed Y.N., Arya B.C., Banerjee T., Begam G.R., Baruah B.P., et al.: Atmospheric fine and coarse mode aerosols at different environments of India and the Bay of Bengal during Winter-2014: implications of a coordinated campaign. *MAPAN J. Metrol. Soc. India.* **29**(4), 273–284 (2014)
- Sharma S.K., Kumar M., Rohtash, Gupta N.C., Saraswati, Saxena M., Mandal T.K.: Characteristics of ambient ammonia over Delhi, India. *Meteorol. Atmos. Phys.* **124**, 67–82 (2014)
- Xia X., Li Z., Holben B., Wang P., Eck T., et al.: Aerosol optical properties and radiative effects in the Yangtze Delta region of China. *J. Geophys. Res.* **112**, D22S12 (2007)